Available online at www.sciencedirect.com

ScienceDirect

Journal of Magnesium and Alloys 9 (2021) 90–101

www.elsevier.com/locate/jma

# A new die-cast magnesium alloy for applications at higher elevated temperatures of 200–300 °C

Xixi Dong[a,*], Lingyun Feng[a], Shihao Wang[a], Eric A. Nyberg[a,b], Shouxun Ji[a,*]

[a] *Brunel Centre for Advanced Solidification Technology (BCAST), Brunel University London, Uxbridge UB8 3PH, United Kingdom*
[b] *Tungsten Parts Wyoming, Laramie, WY 82072, USA*

Received 11 June 2020; received in revised form 17 September 2020; accepted 27 September 2020
Available online 3 November 2020

**Abstract**

The development of lightweight magnesium (Mg) alloys capable of operating at elevated temperatures of 200–300 °C and the ability of using high pressure die casting for high-volume manufacturing are the most advanced developments in manufacturing critical parts for internal combustion engines used in power tools. Here we report the microstructure and mechanical properties of a newly developed die-cast Mg–RE(La,Ce,Nd,Gd)–Al alloy capable of working at higher elevated temperatures of 200–300 °C. The new alloy delivers the yield strength of 94 MPa at 300 °C, which demonstrates a 42% increase over the benchmark AE44 high temperature die-cast Mg alloy. The new alloy also has good stiffness at elevated temperatures with its modulus only decreasing linearly by 13% from room temperature up to 300 °C. Thermal analysis shows a minor peak at 364.7 °C in the specific heat curve of the new alloy, indicating a good phase stability of the alloy up to 300 °C. Nd and Gd have more affinity to Al for the formation of the minority of divorced Al–RE(Nd,Gd) based compounds, and the stable Al-poor $Mg_{12}RE(La_{0.22}Ce_{0.13}Nd_{0.31}Gd_{0.31})Zn_{0.39}Al_{0.13}$ compound acts as the continuous inter-dendritic network, which contribute to the high mechanical performance and stability of the new die-cast Mg alloy at 200–300 °C.


*Keywords:* Magnesium alloys; High pressure die casting; Elevated temperatures; Microstructure; Mechanical properties.

## 1. Introduction

Key components of small internal combustion (IC) engines used in power tools require light-weight materials that are excellent in noise reduction, good damping properties and capable of working at elevated temperatures of 200–300 °C [1,2]. The lightweight piston and cylinder are not only desirable for decreasing the machine vibration and carrying comfort during use, but also increases control and fuel efficiency. Moreover, the massive consumption of these products with small IC engines demands a cost-effective manufacturing method. Therefore, the application of lightweight magnesium alloys that can be high pressure die cast for high volume manufacturing becomes very attractive to industry.

High pressure die casting (HPDC) is a highly efficient and cost-effective precision manufacturing method for the massive production of Mg and/or aluminium (Al) alloy parts in different sectors of industry. Currently, about 90% of cast Mg alloys are manufactured by HPDC [3–6]. However, there are no die-cast Mg alloys currently available on the market for applications at higher elevated temperatures of above 200 °C and ideally up to 300 °C. The challenges are mainly the conflicting requirements between mechanical performance and phase stability at elevated temperatures and die castability. Several Mg-rare earth (RE) based sand casting or permanent-mould casting alloys have been developed and used in industry for applications at 200 °C or above [7], including WE43/54 [8–10], AM-SC1 [11,12], Elektron 21 [13] etc. However, these alloys are not suitable for HPDC because they

* Corresponding authors.
*E-mail addresses:* xixi.dong@brunel.ac.uk (X. Dong), shouxun.ji@brunel.ac.uk (S. Ji).

https://doi.org/10.1016/j.jma.2020.09.012

are prone to form defects such as hot-tearing and die soldering or brittleness in the components produced by HPDC [14].

In the early stage of development of die-cast Mg alloys for high temperature applications, significant amount of Al was used for the improvement of die castability, and a group of Mg–Al based die-cast alloys were developed [7,15]. Representative alloys are the widely used AZ91 and AM60 alloys, the Mg–Al–Si alloys (AS21X, AS31, AS41) [16,17], the Mg–Al–Ca alloy (AX51, AX52) [18], the Mg–Al–Sr alloy (AJ52) and the Noranda alloy Mg–6Al–2Sr–Ca (AJ62X) [19–21], the Mg–Sr–Ca alloy (AJX500) [7], the General Motors alloy Mg–Al–Ca–Sr (AX52J, AXJ530, AXJ531) [22,23], the Mg–9Al–1Ca–Sr alloy (MRI153A) [24], the Mg–8Al–1Ca–Sr alloy (MRI153M) [25,26], the Mg–6.5Al–2Ca–1Sn–Sr alloy (MRI230D) [27–29], the Nissan alloy Mg–Al–Ca–RE [30], the Honda alloy Mg–5Al–2Ca–2RE (ACM522) [31], the Mg–0.5Zn–6Al–1Ca–3RE alloy (ZACE05613) and the Mg–0.5Zn–4Al–1Ca–1RE alloy (ZACE05411) [32], the Mg–4Al–RE (La, Ce) alloys (AE42, AE44) [33–35], the Mg–Al–Ba–Ca alloy [36], etc. The general working temperature of these Mg–Al based die-cast alloys is at a level of ~150 °C, due to the formation of the low melting point Al-rich phases that are unstable when temperatures are close to or higher than 175 °C [7,37,38]. The AX52J, MRI230D and ACM522 alloys with the presence of 2 wt.% Ca can work at a slightly higher temperature of ~180 °C [14,15]. The AE44 alloy for the applications at 150 °C is a major achievement among the Mg–Al based die-cast alloys with good combination of die castability, mechanical properties at elevated temperatures, and good corrosion resistance [35,39]. In recent years, the addition of Al is a concern, and few Al-free die-cast Mg alloys were developed for applications at elevated temperatures [14]. The Al-free die-cast Mg–2.5RE–0.35Zn alloy (MEZ) was developed with good creep resistance, but the ductility and strength of the alloy were low [40]. The Al-free die-cast Mg–RE–Zr–Zn alloys were well investigated with medium as-cast strength [41,42]. An die-cast Mg–4 wt.%RE (La,Ce,Nd) alloy named HP2+ for commercialisation was developed with the presence of impurity level of ~0.05 wt.%Al [14,43–45]. The Al-free HP2+ die-cast Mg alloy delivers higher mechanical performance especially creep resistance at elevated temperatures, which is a significant achievement and promising for the applications at 150–200 °C [14,45]. However, 4 wt.% RE is near the maximum of Al-free die-cast Mg–RE alloys, and further addition of RE for higher working temperatures and elevated mechanical performance will make the Al-free die-cast Mg–RE alloys too brittle, with hot-tearing or die-soldering occurring during die-casting [14].

In this work, different from the existing die-cast Mg alloys using Al-rich or Al-free in development, a new design for elevated die-cast Mg alloys was adopted, in which an appropriate addition of Al as a minor element was proposed to enhance the addition of RE for higher elevated performance without losing die castability of alloy, and a new Mg–5 wt.%RE(La,Ce,Nd,Gd)–Al die-cast Mg alloy was developed for applications at higher elevated temperatures of 200–300 °C. The microstructure, mechanical performance and phase stability of the new alloy were studied.

Table 1
Measured chemical composition of the newly developed die-cast Mg–RE–Al alloy.

| Element | La | Ce | Nd | Gd | Al | Zn | Mn | Y | Mg |
|---|---|---|---|---|---|---|---|---|---|
| wt.% | 1.62 | 0.89 | 0.91 | 1.38 | 0.52 | 0.32 | 0.24 | 0.09 | Bal. |

## 2. Material and methods

### 2.1. Alloy preparation

An electric resistance furnace embedded with a steel crucible was used for melting. A mixed gas of $N_2$ (6 L/min) and $SF_6$ (0.025 L/min) was applied for protection during melting. To make the required composition of the new alloy listed in Table 1, pure Mg ingot was first melted, then the other alloy elements were added via the addition of pure Al, pure Zn and the master alloys of Mg–30 wt.%La, Mg–30 wt.%Ce, Mg–30 wt.%Nd, Mg–30 wt.%Gd, Mg–30 wt.%Y and Mg–5 wt.%Mn. The two representative high temperature die-cast Mg alloys of AE44 (Mg4.0Al2.8Ce1.2La0.2Mn, in wt.%) and HP2+ (Mg1.6La1.0Ce1.0Nd0.45Zn0.05Al, in wt.%) were also melted and die-cast for making comparison sample. The melts were controlled at 720 °C and held for 30 min before HPDC.

### 2.2. HPDC and mechanical testing

The die-cast Mg alloy melts were loaded manually into the shot sleeve of a 4500 kN cold chamber high-pressure die-casting machine. Fig. 1a displays a schematic view of the HPDC of the die-cast Mg alloys. Fig. 1b presents a schematic showing the configuration of the steel die used for die-casting the ASTM B557 standard round mechanical test bars with a gauge diameter of $\phi$6.35 mm and a gauge length of 50 mm. During HPDC, the die was preheated at 225 °C, and the melts were poured at 715 °C, while the intensification pressure was set at 320 bar and the shot sleeve diameter was 70 mm. The $\phi$6.35 mm die-cast bars were subjected to tensile tests at ambient temperature and elevated temperatures of 150 °C, 250 °C and 300 °C, using an Instron mechanical testing machine. ASTM E8/E8M and ASTM E21 standards were followed for ambient tensile tests and high temperature tensile tests, respectively. The ramp rate for ambient tensile tests was controlled at 1 mm/min, and the straining rate for high temperature tensile tests was maintained at 0.0002/s. For each alloy, twelve samples were pulled at ambient temperature, and six samples were pulled at each elevated temperature, to give the average tensile properties with standard deviations. Density measurements were conducted on a laboratory balance utilizing Archimedes' principle, and the mass of the test sample in air and water was measured to determine the density.

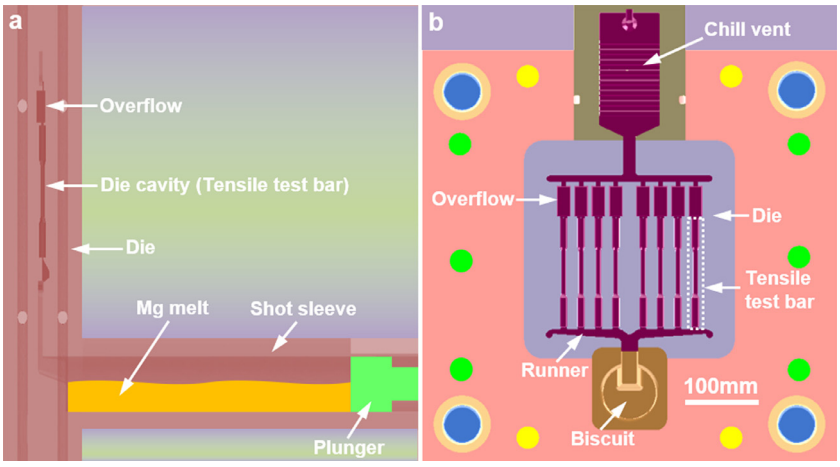


Fig. 1. High pressure die casting of the developed BDM1 die-cast Mg alloy. (a) Main view showing the injection of the Mg melt into the die cavity for the formation of the mechanical test samples. (b) Left view showing the die used for the formation of the mechanical test samples.

### 2.3. Modulus test and thermal analysis

The Young's modulus of the developed new alloy was conducted on a RFDA HT1600 machine from room temperature up to 350 °C. Rectangular shaped samples with dimensions of 40 mm (*L*) x 12 mm (*W*) x 2 mm (*D*) were used for modulus testing. The modulus data was obtained during both heating and cooling cycles, in which both the heating rate and the cooling rate were set at 3 °C/min, while the modulus data was collected every minute. The thermal analysis of the new alloy was conducted on a differential scanning calorimetry (DSC) machine from room temperature up to 700 °C with the protection of nitrogen, and the heating rate was 5 °C/min, while the specific heat of the new alloy was recorded every 0.16 °C.

### 2.4. Microstructure analysis

Scanning electron microscope (SEM) and transmission electron microscope (TEM) were used for microstructure characterization. SEM analysis was performed at 20 kV for morphological observation and element mapping. Ion polishing was used to fabricate TEM samples, after grinding to a ~50 μm thick $\phi$3 mm disc. High accuracy energy dispersive X-ray spectroscopy (EDS) under scanning transmission electron microscopy (STEM) was applied for composition analysis of phases.

## 3. Results and discussion

### 3.1. New die-cast Mg–RE–Al alloy

The measured chemical composition of the newly developed die-cast Mg–RE–Al alloy is shown in Table 1, and the composition range of the new alloy can be found in the authors' recent patent [46]. The low solid solubility RE elements La and Ce was reported beneficial for die castability of Mg alloys, as these two elements, especially La, help narrow the solid-liquid solidification temperature range that is important for die-casting [14], and the presence of ~2.5 wt.%(La+Ce) could act as the cast base of the Mg–RE–Al alloy. The higher solid solubility RE elements Nd and Gd are helpful for strengthening at ambient temperature and at elevated temperatures for die-cast Mg alloys [47,48]. For Al-free die-cast Mg–RE alloys, when the total amount of RE elements is more than 4 wt.%, the alloys was thought too brittle and/or hot-tearing for die-casting [14]. Therefore, the addition of ~2.5 wt.%(La+Ce) can at most tolerate an extra addition of less than 1.5 wt.%(Nd, Gd), without the addition of Al.

In the meantime, Al in Mg alloys is well-known beneficial for die castability [45], but excessive addition deteriorates the mechanical performance at elevated temperatures and limits the working temperature to ~175 °C [37–39]. In fact, an appropriate amount of Al addition can enable a higher amount of RE element without fully losing the die castability of Mg–RE alloys, as disclosed in this work. For example, the appropriate addition of ~0.5 wt.%Al allows the addition of ~2.5 wt.%(Nd, Gd) in the newly developed Mg–RE–Al alloy. This means that the total amount of RE elements in the newly developed Mg–RE–Al alloy can be ~5.0 wt.% with suitable castability in HPDC. Moreover, the addition of Zn was reported beneficial for the improvement of the mechanical performance at elevated temperatures [14], via the refinement of the RE-containing precipitates in Mg matrix [49]. The addition of Mn is helpful for the neutralization of impurity elements such as Fe and the improvement of corrosion resistance [50]. The minor addition of Y helps to improve melt stability [14]. Consequently, the final composition of the developed Mg–RE–Al alloy can provide a good combination of die castability and mechanical properties at both ambient and elevated temperatures, as discussed in Section 3.4.

The porosity level in the die-cast tensile bars of the newly developed die-cast Mg–RE–Al alloy was determined as 0.28%, via density measurements the alloy under gravity casting and high pressure die casting, basing on the Archimedes'

Table 2
Porosity in the die-cast tensile bars of the newly developed die-cast Mg–RE–Al alloy via density measurement.

| Casting method | Test No. | $M_{Air}$ (g) | $M_{Water}$ (g) | Density (g/cm$^3$) | Porosity (%) |
|---|---|---|---|---|---|
| Gravity casting | 1 | 134.2 | 60.03 | 1.809 | 0 (Reference) |
| High pressure die casting | 1 | 11.06 | 4.93 | 1.804 ± 0.0003 | 0.28 ± 0.02 |
| | 2 | 11.33 | 5.05 | | |
| | 3 | 11.55 | 5.15 | | |

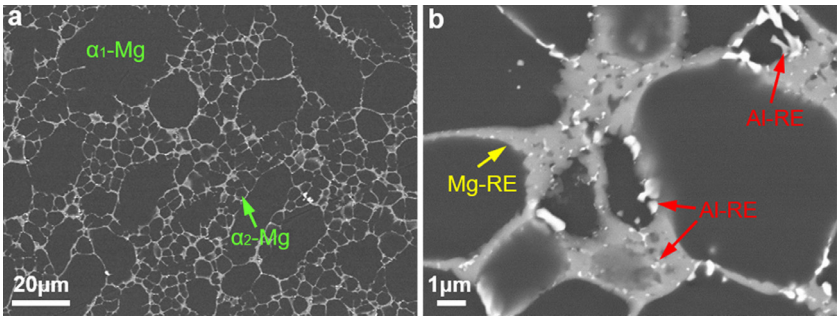


Fig. 2. SEM morphology of the newly developed die-cast Mg–RE–Al alloy in the as-cast state. (a) Low magnification morphology showing the primary $\alpha_1-$Mg phase nucleated in the shot sleeve and the secondary $\alpha_2-$Mg phase nucleated in the die cavity, (b) High magnification morphology showing the Mg–RE and Al–RE based compounds at the grain boundaries.

principle, as shown in Table 2. The microstructure of the gravity casting sample can be referenced as porosity-free, and the porosity level in the die-cast tensile bars was calculated basing on the density difference to the gravity casting condition. The porosity level in commercial die-cast Mg alloys for elevated applications was generally reported above 1% [36], and the low porosity level here can reflect the suitability of the alloy in high pressure die casting.

It should be mentioned that the reduction or avoiding of RE in magnesium alloys is a preference in recent years, as RE is mainly imported from very limited countries and the cost of RE is very volatile. Currently, 4 wt.% RE are added in the two representative high temperature die-cast Mg alloys AE44 and HP2+, however, it is hard for these alloys to work at elevated temperatures above 200 °C with the presence of 4 wt.% RE. The addition of a higher level of ~5 wt.% RE is the very limited choice, to enable the present developed Mg–RE–Al alloy to work at higher elevated temperatures of 200–300 °C, for demanding applications such as the critical parts in small internal combustion engines. Explorations are encouraged on this demanding topic in near future, to enable die-cast Mg alloys work at elevated temperatures of up to 300 °C with less or without addition of RE.

### 3.2. SEM morphology

Fig. 2 shows SEM morphology of the newly developed die-cast Mg–RE–Al alloy in as-cast state. Fig. 2a presents the morphology at a low magnification view. The Mg matrix phase has two different grain sizes, i.e., the primary $\alpha_1-$Mg phase with size of ~20–50 μm and the secondary $\alpha_2-$Mg phase with size of ~2–10 μm. The $\alpha_1-$Mg phase nucleated in the shot sleeve with lower cooling rate, so it was larger in size than the $\alpha_2-$Mg phase that nucleated in the die cavity with higher cooling rate [51]. Network of the other phases was found at the grain boundaries of Mg matrix phase. Fig. 2b shows the morphology at high magnification of the grain boundary network shown in Fig. 2a. The main body of the network is continuous solid compound, which is different from the continuous network of lamellar $Al_{11}RE(La,Ce)_3$ eutectic observed in the AE44 die-cast alloy with significant addition of 4 wt.%Al [37–39].

In the new Mg–RE–Al alloy, the continuous solid compound that makes up the majority of the network is Mg–RE based compound, while the divorced compounds that take the minority of the network are Al–RE based compounds, which have been verified by STEM analysis in Section 3.3. The Al–RE based compounds display two kinds of morphologies, i.e., a petaloid shape and a blocky shape.

Fig. 3 displays the SEM elemental distribution map of the newly developed die-cast Mg–RE–Al alloy in the as-cast state. Fig. 3a is the SEM micrograph of the area mapped, and Fig. 3b–i shows the elemental mapping of Mg, Mn, La, Ce, Zn, Al, Nd and Gd in Fig. 3a, respectively. The concentration of La, Ce, Nd, Gd and Zn at the grain boundaries was observed in the Mg–RE compound, while Al was found depleted in the Mg–RE compound, which demonstrate that the Mg–RE compound is a Mg–RE(La,Ce,Nd,Gd)–Zn based phase. From Fig. 3g, the enrichment of Al was observed in the blocky Al–RE compound. According to Fig. 3h and i, the enrichment of RE elements Nd and Gd was also found in the blocky Al–RE compound, which shows that the blocky Al–RE compound is Al–RE(Nd,Gd) based phase. The mapping results in Fig. 3 also reveal that Nd and Gd have more affinity to Al for the formation of Al–RE(Nd,Gd) based compounds in the newly developed alloy.

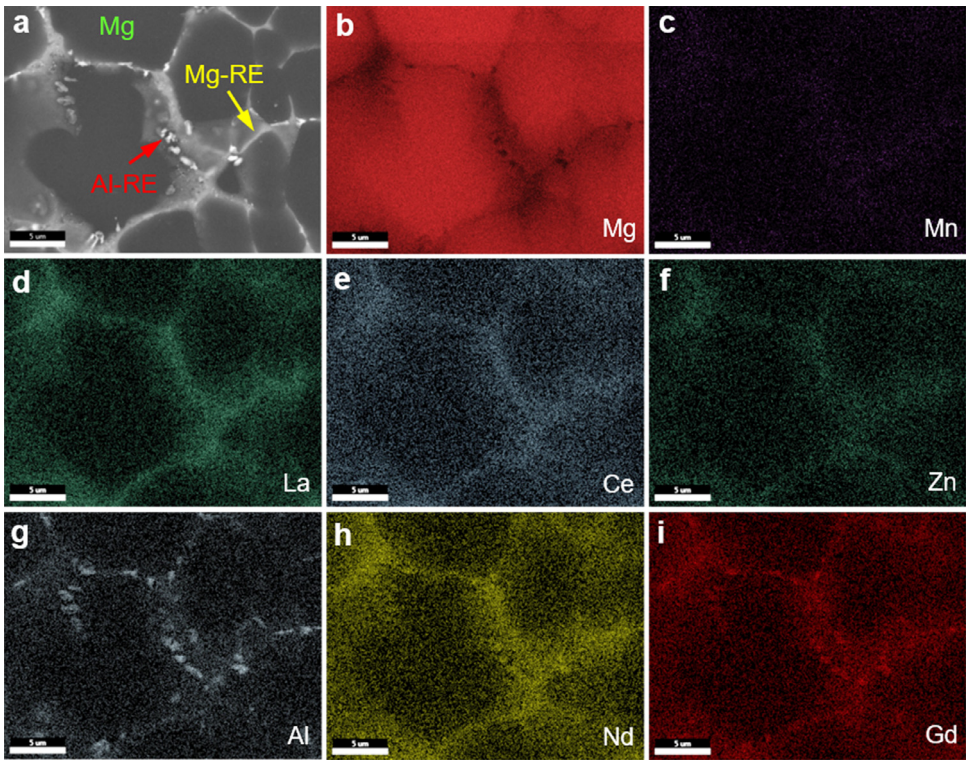


Fig. 3. SEM mapping of elemental distribution in the newly developed die-cast Mg–RE–Al alloy in the as-cast state. (a) SEM micrograph showing the mapping area, (b–i) mapping of elements (b) Mg, (c) Mn, (d) La, (e) Ce, (f) Zn, (g) Al, (h) Nd and (i) Gd.

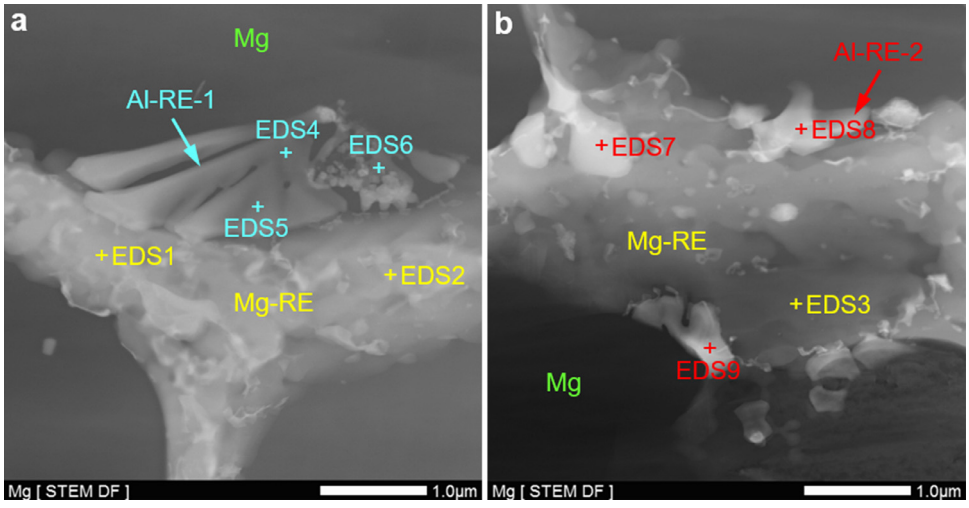


Fig. 4. High magnification STEM images showing the microstructure of the newly developed die-cast Mg–RE–Al alloy in as-cast state. (a) STEM morphology of the continuous Mg–RE based compound and the petaloid Al–RE based compound 1, (b) STEM morphology of the blocky Al–RE based compound 2.

### *3.3. TEM confirmation*

STEM was applied to further confirm the features in the newly developed die-cast Mg–RE–Al alloy. Fig. 4 presents high magnification STEM images showing the microstructure of the new alloy in as-cast state. In addition to the continuous Mg–RE based compound, two kinds of divorced Al–RE based compounds were observed at the grain boundaries of the Mg matrix under STEM analysis, i.e., the petaloid Al–RE based compound 1 and the blocky Al–RE based compound 2, which corresponds with the SEM observation in Fig. 2b. Fig. 4a shows typical STEM morphology of the continuous Mg–RE based compound and the petaloid Al–RE based compound 1. Fig. 4b presents the representative STEM morphology of the blocky Al–RE based compound 2. In order to determine the Mg–RE based compound and the two Al–RE based compounds, high accuracy EDS analysis was applied under STEM to determine the chemical compositions of the compounds. Each of the Mg–RE based compound and the two Al–RE based compounds were

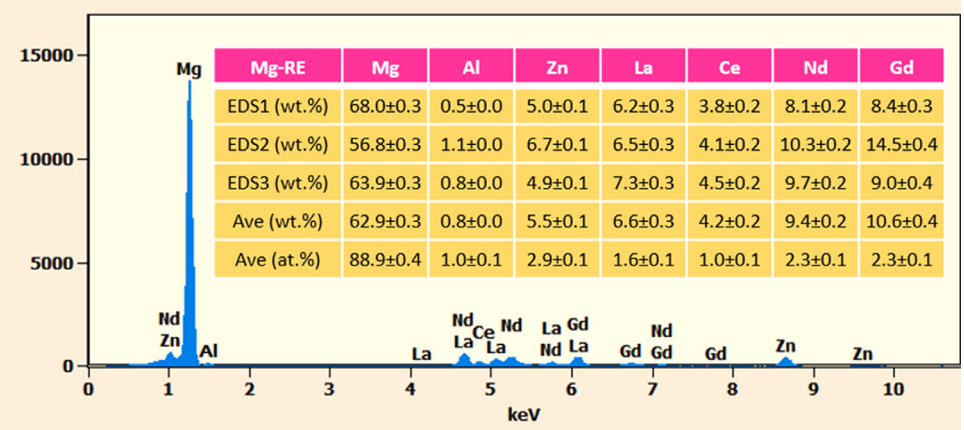


| Mg-RE | Mg | Al | Zn | La | Ce | Nd | Gd |
|---|---|---|---|---|---|---|---|
| EDS1 (wt.%) | 68.0±0.3 | 0.5±0.0 | 5.0±0.1 | 6.2±0.3 | 3.8±0.2 | 8.1±0.2 | 8.4±0.3 |
| EDS2 (wt.%) | 56.8±0.3 | 1.1±0.0 | 6.7±0.1 | 6.5±0.3 | 4.1±0.2 | 10.3±0.2 | 14.5±0.4 |
| EDS3 (wt.%) | 63.9±0.3 | 0.8±0.0 | 4.9±0.1 | 7.3±0.3 | 4.5±0.2 | 9.7±0.2 | 9.0±0.4 |
| Ave (wt.%) | 62.9±0.3 | 0.8±0.0 | 5.5±0.1 | 6.6±0.3 | 4.2±0.2 | 9.4±0.2 | 10.6±0.4 |
| Ave (at.%) | 88.9±0.4 | 1.0±0.1 | 2.9±0.1 | 1.6±0.1 | 1.0±0.1 | 2.3±0.1 | 2.3±0.1 |

Fig. 5. STEM-EDS results of the continuous Mg–RE based compound in the newly developed die-cast Mg–RE–Al alloy based on the STEM analysis in Fig. 4.

measured at three local points by EDS, as shown in Fig. 4a and b.

Fig. 5 shows the STEM-EDS results of the continuous Mg–RE based compound in the newly developed die-cast Mg–RE–Al alloy. EDS1 and EDS2 were taken from the Mg–RE based compound in Fig. 4a, and EDS3 was taken from the Mg–RE based compound in Fig. 4b. Results of EDS1, EDS2 and EDS3 are consistent with each other, which confirms that the composition of the Mg–RE based compound can be described by the average value as $Mg_{88.9}La_{1.6}Ce_{1.0}Nd_{2.3}Gd_{2.3}Zn_{2.9}Al_{1.0}$, namely, $Mg_{12}RE(La_{0.22}Ce_{0.13}Nd_{0.31}Gd_{0.31})Zn_{0.39}Al_{0.13}$. $Mg_{12}RE(Zn)$ was reported as the main compound in the Mg–RE(La,Ce,Nd) based alloys [14,45], which agrees with the observation in the present developed new alloy.

Fig. 6a presents the STEM-EDS results of the petaloid Al–RE based compound 1 in the newly developed Mg–RE–Al alloy. EDS4, EDS5 and EDS6 were taken from the petaloid compound shown in Fig. 4a. The consistency of the three EDS results indicates that the petaloid Al–RE based compound can be represented as $Mg_{93.4}Al_{3.2}La_{0.4}Ce_{0.3}Nd_{1.0}Gd_{1.4}Zn_{0.3}$, i.e., $Mg_{30.1}Al_{1.03}RE(La_{0.13}Ce_{0.1}Nd_{0.32}Gd_{0.45})Zn_{0.1}$. Fig. 6b shows the STEM-EDS results of the blocky Al–RE based compound 2 in the newly developed Mg–RE–Al alloy. EDS7, EDS8 and EDS9 were taken from three blocky Al–RE based compounds shown in Fig. 4b. The results suggest that the blocky Al–RE based compound can be described as $Mg_{50.4}Al_{24.1}La_{2.4}Ce_{1.5}Nd_{8.2}Gd_{10.5}Zn_{2.9}$, namely, $Mg_{2.2}Al_{1.07}RE(La_{0.11}Ce_{0.07}Nd_{0.36}Gd_{0.46})Zn_{0.13}$.

The above-mentioned STEM-EDS composition analysis results show that the atomic ratio of Mg:RE in the Mg–RE compound is ~12:1, and the atomic ratio of Al:RE in the Al–RE compound is ~1:1. Selected area electron diffraction (SAED) was also conducted under TEM, for the identification of the Mg–RE and Al–RE compounds. The $Mg_{12}RE$ (RE=La, Ce, Nd or Gd) phase was reported having the tetragonal unit cell ($a=1.03$ nm, $c=0.60$ nm) [52]. The $Al_2RE_3$ (RE=Gd) phase was reported having the tetragonal unit cell ($a=0.83$ nm, $c=0.77$ nm) [53]. Fig. 7a shows the SAED pattern of the Mg–RE compound, and it matches well with the SAED pattern of the $Mg_{12}Ce$ phase along the [111] zone axis. Fig. 7b presents the SAED pattern of the Al–RE compound, and it fits well with the SAED pattern of the $Al_2Gd_3$ phase along the [−122] zone axis.

Combining the STEM-EDS composition analysis results and the SAED results, the Mg–RE compound was identified as the $Mg_{12}RE$ (RE=La, Ce, Nd, Gd) phase, while the Al–RE compound was identified as the $Al_2RE_3$ (RE=La, Ce, Nd, Gd) phase. From Figs. 2–4, the Al–RE compound is small, so there should be error in the STEM-EDS composition analysis of the Al–RE compound, which results in the minor difference of the atomic ratio of Al:RE given by STEM-EDS analysis and SAED analysis. Zn atom was reported can present in the RE-containing phases in Mg–RE alloys without changing the unit cell of RE-containing phases [52,54], and this can explain the detection of small amount of Zn in the present $Mg_{12}RE$ and $Al_2RE_3$ compounds by STEM-EDS composition analysis.

### 3.4. Tensile properties at elevated temperatures

Fig. 8a–d shows the typical tensile stress-strain curves of the newly developed die-cast Mg–RE–Al alloy at ambient temperature and elevated temperatures of 150 °C, 250 °C and 300 °C, respectively. The results are compared with the two existing and representative high temperature die-cast Mg alloys, the AE44 alloy with significant addition of 4 wt.%Al and the Mg–RE based HP2+ alloy with the addition of ~4 wt.%RE(La,Ce,Nd). The tensile results are based on the $\phi$6.35 mm die-cast bars with the same casting condition. The newly developed Mg–RE–Al alloy with the addition of ~5 wt.%RE(La,Ce,Nd,Gd) and ~0.5 wt.%Al always shows higher yield strength than both the AE44 and HP2+ alloys, at ambient and elevated temperatures, and the ambient ductility of the new alloy is slightly higher than that of the HP2+ alloy, which verify the alloy design principle introduced in this work that appropriate addition of Al in die-cast Mg–RE based alloy can enhance the tolerable addition of RE for ambient

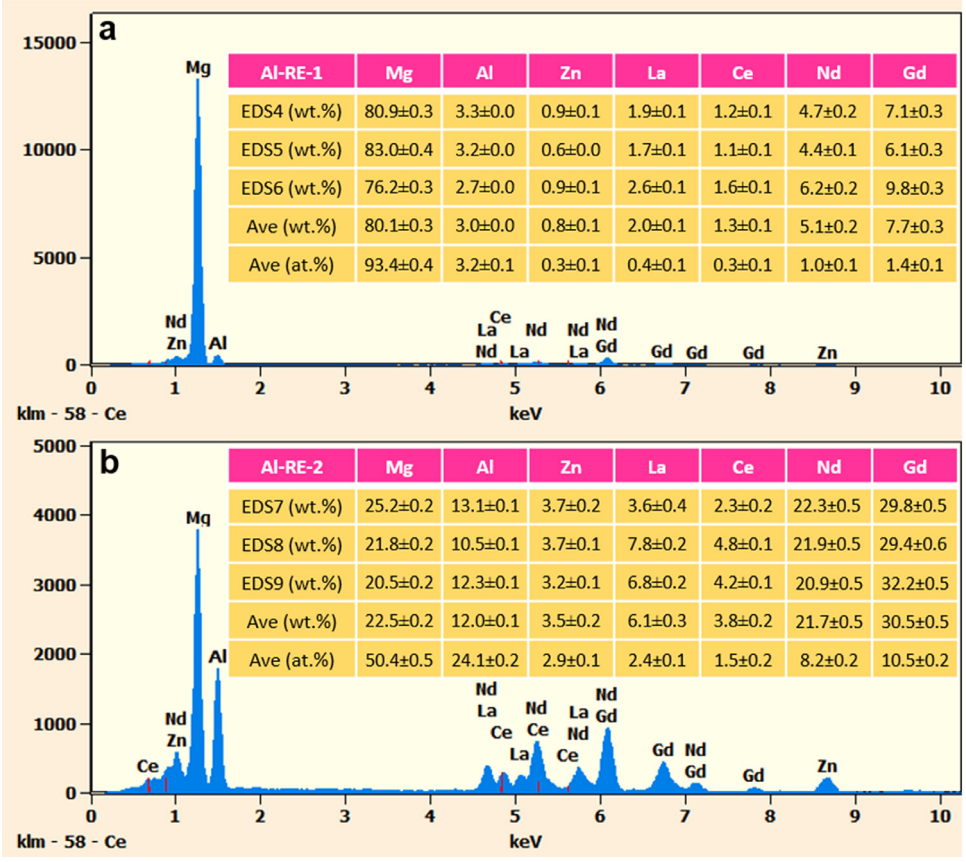


Fig. 6. STEM-EDS results of (a) the petaloid Al–RE based compound 1 and (b) the blocky Al–RE based compound 2 in the newly developed die-cast Mg–RE–Al alloy based on the STEM analysis in Fig. 4.

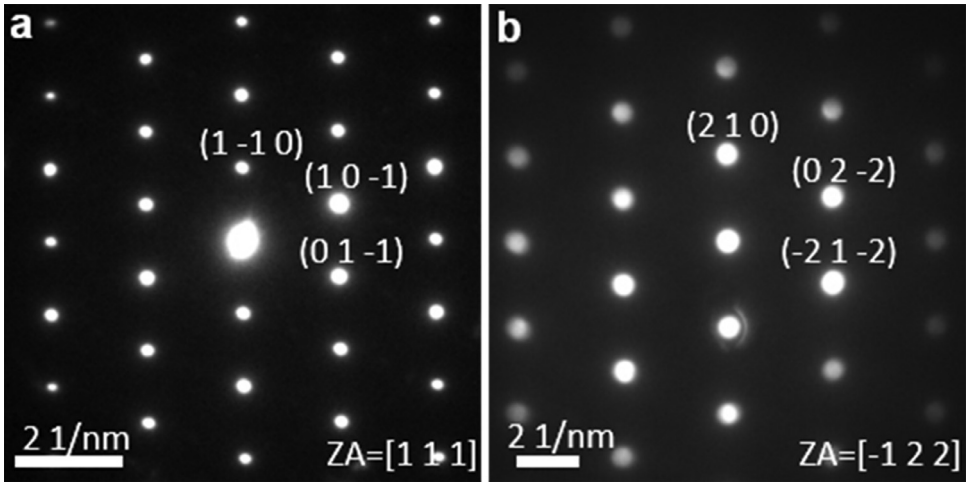


Fig. 7. Selected area electron diffraction patterns of (a) Mg–RE compound and (b) Al–RE compound in the newly developed die-cast Mg–RE–Al alloy.

and elevated strengthening without losing the die castability and ductility of the alloy.

Fig. 9a–c presents the statistical mean yield strength (YS), ultimate tensile strength (UTS) and elongation of the newly developed die-cast Mg–RE–Al alloy at ambient temperature and elevated temperatures of 150 °C, 250 °C and 300 °C, respectively, in comparison with the two existing and representative high temperature die-cast Mg alloys AE44 and HP2+. The measured YS of the new alloy is 170±2.8 MPa at room temperature, and it is 32% and 17% higher than that of the AE44 and HP2+ alloys, respectively. At 300 °C, the YS of the new alloy is 94 ± 1.8 MPa, which is 42% and 20% higher than that of the AE44 and HP2+ alloys, separately. From Fig. 9b, the UTS of the new alloy is higher than the AE44 alloy at elevated temperatures of 150 °C and above, and it is higher than the HP2+ alloy

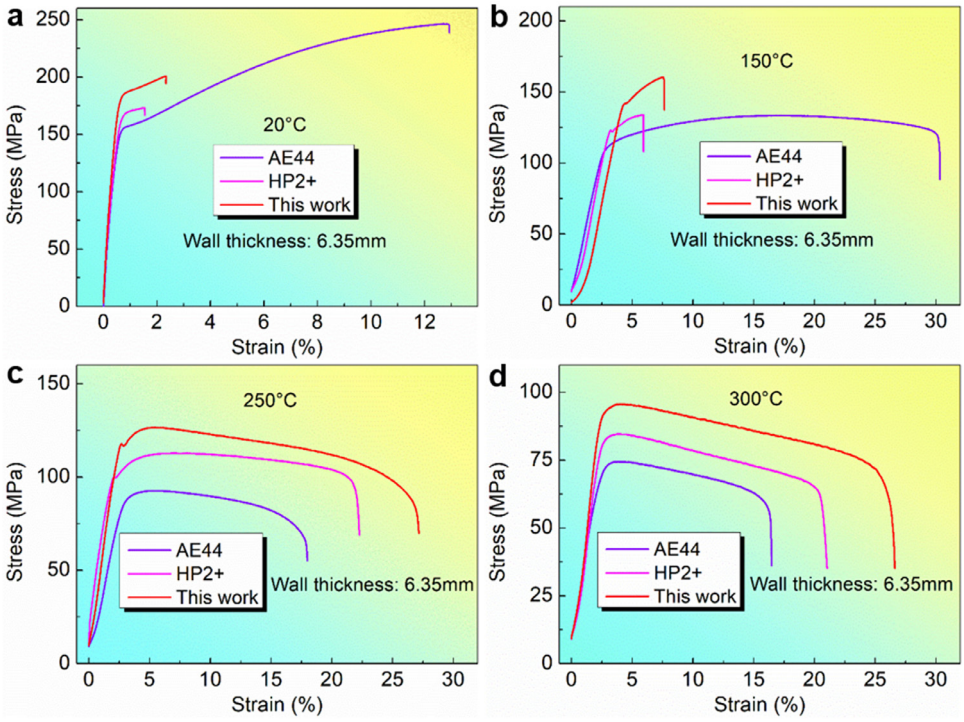


Fig. 8. Typical tensile stress-strain curves of the newly developed die-cast Mg–RE–Al alloy at ambient and elevated temperatures and compared to the existing AE44 and HP2+ high temperature die-cast Mg alloys at (a) ambient temperature (20 °C), (b) 150 °C, (c) 250 °C, (d) 300 °C.

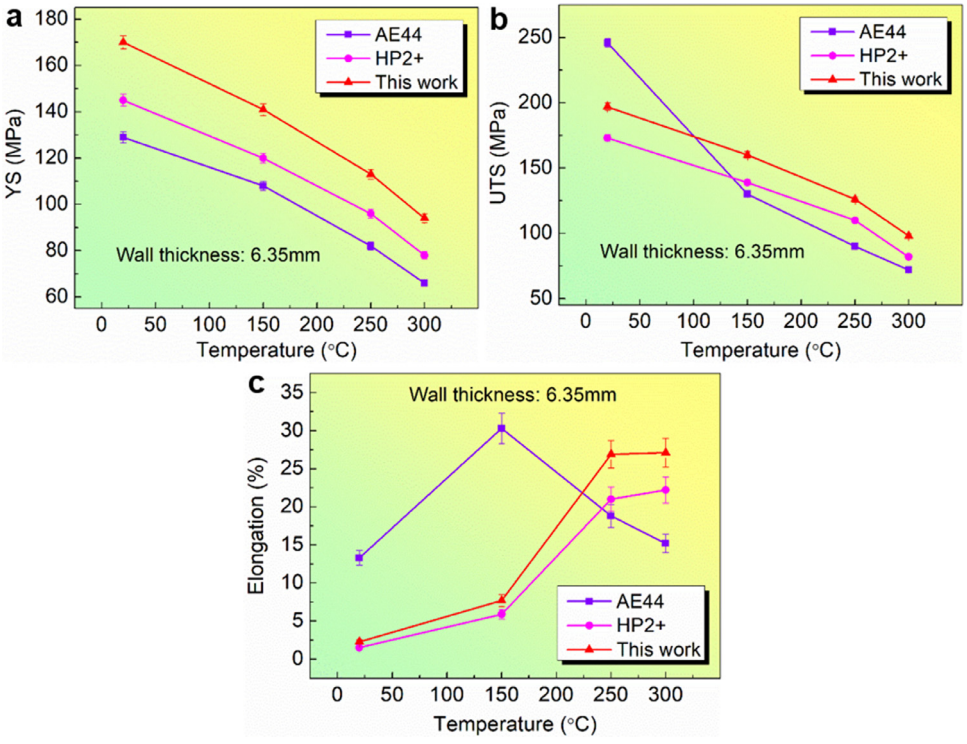


Fig. 9. Statistical mean tensile properties of the newly developed die-cast Mg–RE–Al alloy at ambient and elevated temperatures and compared with the existing AE44 and HP2+ high temperature die-cast Mg alloys. (a) Yield strength, (b) Ultimate tensile strength, (c) Elongation.

Table 3
Detail data for the mean tensile properties of the investigated die-cast Mg alloys at ambient and elevated temperatures with standard deviations.

| Alloy | Tensile properties | 20 °C | 150 °C | 250 °C | 300 °C |
|---|---|---|---|---|---|
| AE44 | YS (MPa) | 129 ± 2.4 | 108 ± 2.0 | 82 ± 1.7 | 66 ± 1.4 |
| | UTS (MPa) | 246 ± 3.2 | 130 ± 2.0 | 90 ± 1.7 | 72 ± 1.4 |
| | Elongation (%) | 13.3 ± 1.0 | 30.3 ± 2.0 | 18.8 ± 1.5 | 15.2 ± 1.2 |
| HP2+ | YS (MPa) | 145 ± 2.6 | 120 ± 2.2 | 96 ± 1.9 | 78 ± 1.6 |
| | UTS (MPa) | 173 ± 2.7 | 139 ± 2.2 | 110 ± 1.8 | 82 ± 1.7 |
| | Elongation (%) | 1.5 ± 0.2 | 5.9 ± 0.6 | 21.0 ± 1.6 | 22.2 ± 1.7 |
| Mg–RE–Al | YS (MPa) | 170 ± 2.8 | 141 ± 2.5 | 113 ± 2.1 | 94 ± 1.8 |
| | UTS (Mpa) | 197 ± 2.8 | 160 ± 2.5 | 126 ± 2.0 | 98 ± 1.7 |
| | Elongation (%) | 2.3 ± 0.3 | 7.7 ± 0.8 | 26.9 ± 1.8 | 27.1 ± 1.9 |

at ambient and elevated temperatures. The ductility of the new alloy is 2.3 ± 0.3%, which is lower than the reported Al-containing Mg–Al based die-cast alloys that have a ductility of over 4% [45]. However, both the strength and ductility of the new alloy are higher than Al-free HP2+ alloy. With the increase of the temperature from 150 °C to 250 °C, the considerable increase of the ductility of the new alloy indicates that the thermal activation effect for deformation is more significant at 250 °C, and deformation is much easier at 250 °C than that at 150 °C. The ductility of the new alloy increases to 27.1 ± 1.9% with increasing test temperature up to 300 °C, which is slightly higher than the HP2+ alloy. With the increase of temperature, the ductility of the AE44 alloy initially increases at 150 °C and then decreases afterwards, which indicates the poor stability of the Al-rich eutectic network in the alloy at elevated temperatures of 250 °C and above. Detail data for the mean tensile properties of the new die-cast Mg–RE–Al alloy, the AE44 alloy and the HP2+ alloy with standard deviations is listed in Table 3.

In addition to the AE44 and HP2+ alloys, the tensile properties of other die-cast Mg alloys for elevated applications were well reported at ambient temperature and 150 °C [36,45]. The AS31 alloy has the low YS of 125 MPa and 90 MPa at ambient temperature and 150 °C, respectively, while the alloy has excellent ambient ductility of 13% [45]. The MRI153M and MRI153A alloys have the medium YS of 160 MPa and 125 MPa at ambient temperature and 150 °C, separately, as well as the medium ambient ductility of 7% [45]. The AXJ530 and MRI230D alloys have the high YS of ~180 MPa at ambient temperature in association with the ambient ductility of 4%, while the YS of the two alloys decreases significantly to ~140 MPa at 150 °C [45]. The ambient YS of the new die-cast Mg–RE–Al alloy is lower than the AXJ530 and MRI230D alloys, but the YS of the new alloy is comparable to the AXJ530 and MRI230D alloys at 150 °C. Recently, a die-cast Mg–Al–Ba–Ca alloy was reported with the weight ratio of Al:Ba:Ca as 2:1:1, and the alloy has the YS of 140 MPa, 172 MPa and 202 MPa at ambient temperature, the YS of 111 MPa, 142 MPa and 160 MPa at 150 °C, as well as the ductility of 2.5%, 1.4% and 1.6% at ambient temperature, with the presence of 4 wt.%, 8 wt.% and 12 wt.% alloy elements, respectively [36]. The new die-cast Mg–RE–Al alloy is comparable to the Mg–Al–Ba–Ca alloy in strength,

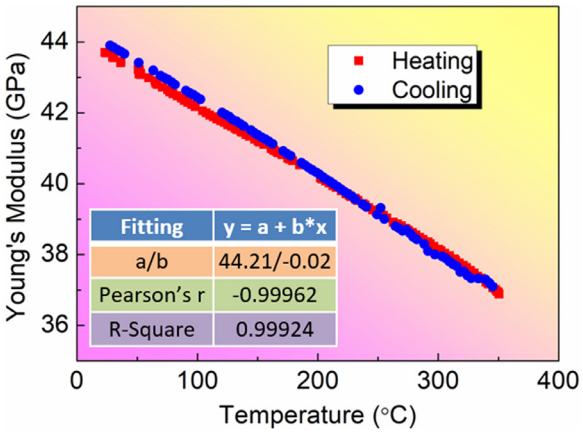


Fig. 10. Relationship between the modulus and the measuring temperatures of the newly developed die-cast Mg–RE–Al alloy during heating and cooling test cycles.

while the ductility of the new alloy is slightly higher than the Mg–Al–Ba–Ca alloy. The new die-cast Mg–RE–Al alloy has higher potential than the existing Al-containing Mg–Al based die-cast alloys and the Al-free Mg–RE alloy HP2+, at the demanding elevated temperatures of 200–300 °C, as the existing die-cast Mg alloys was reported can only work up to 200 °C [14,45].

### 3.5. Young's modulus at elevated temperatures

Fig. 10 shows the Young's modulus of the newly developed die-cast Mg–RE–Al alloy from room temperature (RT) up to 350 °C. The impulse excitation technique was applied to measure the resonant frequencies of the test sample under the inducement of a microphone, and the Young's modulus $E$ is determined as follows:

$$E = 0.9465\left(\frac{mf^2}{W}\right)\left(\frac{L^3}{D^3}\right)K \quad (1)$$

Where $m$, $L$, $W$ and $D$ are the mass, length, width and thickness of the rectangle test sample, respectively, $f$ is measured the flexural frequency, and $K$ is the correction factor.

The modulus of the new alloy decreases linearly with increasing temperatures and increases linearly with decreasing temperatures between RT and 350 °C. More importantly, the

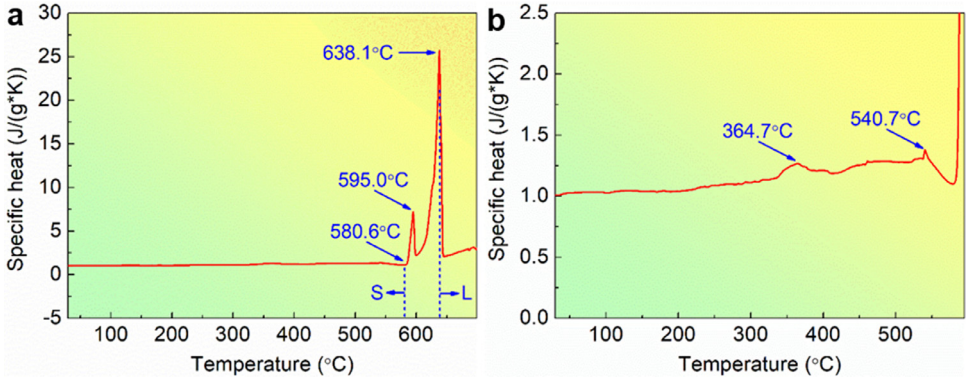


Fig. 11. Thermal analysis curves showing the evolution of the specific heat of the newly developed die-cast Mg–RE–Al alloy versus temperature. (a) Specific heat over the entire measurement temperature range from ambient temperature up to 700 °C. (b) Magnification of (a) showing minor changes of specific heat in the solid stage.

modulus correlates well during the heating and cooling test cycles. The modulus-temperature relation of the new alloy was therefore determined by linear fitting of the average value of the heating and cooling data as follows:

$$E_{BDM1} = 44.21 - 0.02 * T\,(\text{GPa}, \text{RT} \leq T \leq 350^{\circ}\text{C}) \quad (2)$$

Where $T$ is the temperature (°C). The high correlation coefficient of above 0.999 confirms the validity of the linear fitting.

Stiffness is important but seldom was reported for die-cast Mg alloys at elevated temperatures. The ambient modulus (43.7 GPa) of the new alloy agrees with the general data of 40–50 GPa measured for ambient modulus of Mg alloys [55,56]. The measured modulus of the new alloy decreases linearly to 38.2 GPa at 300 °C, which is only 13% lower than its ambient modulus. This demonstrates that the newly developed die-cast Mg–RE–Al alloy has good stiffness holding capability at elevated temperatures.

### 3.6. Thermal analysis and phase stability

Fig. 11a displays the thermal analysis results for the specific heat of the newly developed die-cast Mg–RE–Al alloy from ambient temperature up to 700 °C, which demonstrates that the new alloy is in solid (S) state below 580.6 °C and liquid (L) above 638.1 °C. Fig. 11b is a magnified view the of Fig. 11a. A minor change of specific heat in the solid range of the new alloy is shown with a minor peak observed at 364.7 °C indicating the occurrence of few weak solid phase transition, while the specific heat increases smoothly with increasing temperature before the peak. This confirms the stability of phases in the new alloy at elevated temperatures up to 300 °C.

The newly developed die-cast Mg–RE–Al alloy clearly delivers higher elevated strength than the representative AE44 and HP2+ high temperature die-cast Mg alloys, and it also has good stiffness holding capability and phase stability at elevated temperatures of up to 300 °C. In addition, test results show that the new alloy also has even higher creep resistance than some commercial Al piston alloys at elevated temperatures of up to 300 °C. However, the creep results and mechanisms of the new alloy are quite complex and will be discussed elsewhere later. These results support the alloy design principle introduced in the development of this new die-cast Mg alloy and the validity of the new alloy working at higher elevated temperatures of 200–300 °C. This is different from other approaches, such as a significant addition of 4 wt.%Al in the AE44 alloy, which leads to the formation of a continuous inter-dendritic network of Al-rich lamellar $Al_{11}RE(La,Ce)_3$ eutectic that is unstable at elevated temperatures above 200 °C [7,37–39]. Compared with the Al-free Mg–RE based alloy such as HP2+, the appropriate addition of ~0.5 wt.%Al enhances the tolerable addition of strengthening RE elements Nd and Gd in the newly developed alloy without losing the die castbility and ductility of the new alloy, and Nd and Gd in turn have more affinity to Al for the formation of the divorced Al–RE(Nd,Gd) based compounds that take the minority of the inter-dendritic network in the new alloy, while the majority of the inter-dendritic network in the new alloy is stable continuous Al-poor $Mg_{12}RE(La_{0.22}Ce_{0.13}Nd_{0.31}Gd_{0.31})Zn_{0.39}Al_{0.13}$ compound, which contribute to the high mechanical performance and phase stability of the newly developed die-cast Mg alloy at higher elevated temperatures of 200–300 °C.

## 4. Conclusions

A new die-cast Mg–RE–Al alloy was developed for applications at higher elevated temperatures of 200–300 °C, and the main results are summarized as follows:

(1) The newly developed die-cast Mg–RE–Al alloy delivers a yield strength of 170 ± 2.8 MPa at room temperature and 94 ± 1.8 MPa at 300 °C. The yield strength of the new alloy at 300 °C is 42% and 20% higher than that of the existing and representative high temperature die-cast Mg alloys AE44 and HP2+, respectively.
(2) The new alloy has good stiffness holding capability at higher elevated temperatures of 200–300 °C. The Young's modulus of the new alloy decreases linearly

with increasing temperature as $E = 44.21–0.02^{*}T$ (GPa, $RT \leq T \leq 350\,°C$), and the modulus at 300 °C is decreased only by 13% compared with the ambient modulus.

(3) Thermal analysis shows a minor peak at 364.7 °C in the measured specific heat curve of the new alloy, bellow the solidus temperature, which verifies the phase stability of the new alloy at higher elevated temperatures of 200–300 °C.

(4) Appropriate addition of Al in Mg–RE alloy enhances the allowable addition of RE, enabling higher performance at elevated temperatures without losing die castability, which can be considered a new design principle for die-cast Mg alloys used for higher elevated temperatures. An addition of ~0.5 wt.%Al allows ~2.5 wt.% of RE (Nd,Gd) elements to be added for a total of ~5.0 wt.% of RE(La,Ce,Nd,Gd) in the new alloy.

(5) Nd and Gd in the new alloy have more affinity to Al for the formation of the minority of divorced Al–RE(Nd,Gd) based compounds, and the stable Al-poor $Mg_{12}RE(La_{0.22}Ce_{0.13}Nd_{0.31}Gd_{0.31})Zn_{0.39}Al_{0.13}$ compound acts as the continuous inter-dendritic network, which improves the alloy performance at elevated temperatures.

## Declaration of Competing Interest

The authors declare no conflicts of interest.

## Acknowledgments

Jon Gadd from BCAST is greatly appreciated for the professional assistance of the high pressure die casting experiments.

## References

[1] N. Hort, H. Dieringa, K.U. Kainer, Magnes. Technol. (2018) 349–353.
[2] X.X. Dong, E.A. Nyberg, S. Ji, Magnes. Technol. (2020) 31–36.
[3] A.A. Luo, J. Magnes. Alloy. 1 (2013) 2–22.
[4] M. Easton, S.M. Zhu, M. Gibson, T. Abbott, H.Q. Ang, X.B. Chen, N. Birbilis, G. Savage, Magnes. Technol. (2017) 123–129.
[5] X.X. Dong, H.L. Yang, X.Z. Zhu, S. Ji, J. Alloy. Compd. 773 (2019) 86–96.
[6] L.H. Liu, T. Zhang, Z.Y. Liu, C.Y. Yu, X.X. Dong, L.J. He, K. Gao, X.G. Zhu, W.H. Li, C.Y. Wang, P.J. Li, L.C. Zhang, L.G. Li, Mater. Basel 11 (2018) 2338.
[7] M.O. Pekguleryuz, A.A. Kaya, Adv. Eng. Mater. 5 (2003) 866–878.
[8] J.G. Wang, L.M. Hsiung, T.G. Nieh, M. Mabuchi, Mater. Sci. Eng. A 315 (2001) 81–88.
[9] Y.H. Kang, Z.H. Huang, S.C. Wang, H. Yan, R.S. Chen, J.C. Huang, J. Magnes. Alloy. 8 (2020) 103–110.
[10] J.F. Nie, B.C. Muddle, Scr. Metall. 40 (1999) 1089–1094.
[11] C.J. Bettles, M.A. Gibson, S.M. Zhu, Mater. Sci. Eng. A 505 (2009) 6–12.
[12] Z.M. Li, P.H. Fu, L.M. Peng, E.P. Becker, G.H. Wu, Mater. Sci. Eng. A 565 (2013) 250–257.
[13] A. Kiełbus, J. Achiev, Mater. Manuf. Eng. 20 (2007) 127–130.
[14] M. Easton, M.A. Gibson, S.M. Zhu, T. Abbott, J.F. Nie, C.J. Bettles, G. Savage, Magnes. Technol. (2018) 329–336.
[15] H. Hu, A. Yu, N.Y. Li, J.E. Allison, Mater. Manuf. Process. 18 (2003) 687–717.
[16] J.E. Hillis, S.O. Shook, SAE Tech. Pap. (1989) 890205.
[17] E. Evangelista, E. Gariboldi, O. Lohne, S. Spigarelli, Mater. Sci. Eng. A 387–389 (2004) 41–45.
[18] A.A. Luo, M.P. Balogh, B.R. Powell, Metall. Mater. Trans. A 33A (2002) 567–574.
[19] M.O. Pekguleryuz, E. Baril, Magnes. Technol. (2001) 119–125.
[20] M. Lefebvre, M. Pekguleryuz, P. Labelle, US Patent (2002) 6342180.
[21] E. Baril, P. Labelle, M. Pekguleryuz, JOM 55 (2003) 34–39.
[22] B.R. Powell, V. Rezhets, A.A. Luo, J.J. Bommarito, B.L. Tiwari, US Patent (2001) 6264763.
[23] B.R. Powell, A.A. Luo, V. Rezhets, J.J. Bommarito, B.L. Tiwari, SAE Tech. Pap. (2001) 2001-01-0422.
[24] F. Buch, S. Schumann, H. Friedrich, E. Aghion, B. Bronfin, B.L. Mordike, M. Bamberger, D. Eliezer, Magnes. Technol. (2002) 61–67.
[25] B. Bronfin, E. Aghion, F. Von Buch, S. Schumann, M. Katsir, Magnes. Technol. (2001) 127–130.
[26] E. Aghion, N. Moscovitch, A. Arnon, Mater. Sci. Technol. 23 (2007) 270–275.
[27] E. Aghion, B. Bronfin, F. Von Buch, S. Schumann, H. Friedrich, Magnes. Technol. (2003) 177–182.
[28] E. Aghion, B. Bronfin, F. Von Buch, S. Schumann, H. Friedrich, JOM 55 (2003) 30–33.
[29] E. Aghion, N. Moscovitch, A. Arnon, J. Mater. Eng. Perform. 18 (2009) 912–916.
[30] K. Samato, Y. Yamamoto, N. Sakate, S. Hirabara, European Patent (1997) EP0799901A1.
[31] S. Koike, K. Washizu, S. Tanaka, T. Baba, K. Kikawa, SAE Tech. Pap. (2000) 2000-01-1117.
[32] I.A. Anyanwu, Y. Gokan, S. Nozawa, A. Suzuki, S. Kamado, Y. Kojima, S. Takeda, T. Ishida, Mater. Trans. 44 (2003) 562–570.
[33] B.R. Powell, V. Rezhets, M.P. Balogh, R.A. Waldo, Magnes. Technol. (2001) 175–182.
[34] M.S. Dargusch, K. Pettersen, P. Bakke, K. Nogita, A.L. Bowles, G.L. Dunlop, Int. J. Cast Met. Res 17 (2004) 170–173.
[35] P. Bakke, H. Westengen, Magnes. Technol. (2005) 291–296.
[36] S. Gavras, S.M. Zhu, M.A. Easton, M.A. Gibson, H. Dieringa, Front. Mater. 6 (2019) 262.
[37] B. Mordike, J. Mater. Process. Technol. 117 (2001) 391–394.
[38] A. Kiełbus, J. Achiev. Mater. Manuf. Eng. 20 (2007) 459–462.
[39] S.M. Zhu, J.F. Nie, M.A. Gibson, M.A. Easton, P. Bakke, Metall. Mater. Trans. A 43A (2012) 4137–4144.
[40] I.P. Moreno, T.K. Nandy, J.W. Jones, J.E. Allison, T.M. Pollock, Magnes. Technol. (2002) 111–116.
[41] G. Atiya, M. Bamberger, A. Katsman, Magnes. Technol. (2011) 249–253.
[42] G. Atiya, M. Bamberger, A. Katsman, Int. J. Mater. Res. 103 (2012) 1277–1280.
[43] M.A. Gibson, C.J. Bettles, M.T. Murray, G.L. Dunlop, Magnes. Technol. (2006) 327–331.
[44] T.A. Sweder, T. Abbott, G.L. Dunlop, M.T. Murray, C.J. Bettles, M.A. Gibson, SAE Tech. Pap. (2006) 2006-01-1564.
[45] S.M. Zhu, M.A. Easton, T.B. Abbott, J.F. Nie, M.S. Dargusch, N. Hort, M.A. Gibson, Metall. Mater. Trans. A 46 (2015) 3543–3554.
[46] X.X. Dong, E.N. Nyberg, M. Almgren, S.X. Ji, Swedish Patent (2019) Application No. 1950219-4.
[47] S. Gavras, M.A. Easton, M.A. Gibson, S.M. Zhu, J.F. Nie, J. Alloy. Compd. 597 (2014) 21–29.
[48] M. Bamberger, G. Atiya, S. Khawaled, A. Katsman, Metall. Mater. Trans. A 45A (2014) 3241–3253.
[49] D. Choudhuri, D. Jaeger, M.A. Gibson, R. Banerjee, Scr. Mater. 86 (2014) 32–35.
[50] M.S. Dani, V.J. Rao, I.B. Dave, Int. Adv. Res. J. Sci. Eng. 2 (2015) 71–77.

[51] X.X. Dong, H. Youssef, Y.J. Zhang, H.L. Yang, S.H. Wang, S.X. Ji, Compos. Part B Eng. 177 (2019) 107453.
[52] C.J. Rossouw, C.J. Bettles, T.J. Davis, C.T. Forwood, P.R. Miller, K. Venkatesan, Acta Crystallogr. A 57 (2001) 321–332.
[53] N.C. Baenziger, J.J. Hegenbarth, Acta Cryst. 17 (1964) 620–621.
[54] Z.J. Yu, Y.D. Huang, X. Qiu, G.F. Wang, F.Z. Meng, N. Hort, J. Meng, Mater. Sci. Eng. A 622 (2004) 121–130.
[55] T. Sumitomo, C.H. Cáceres, M. Veidt, J. Light Met. 2 (2002) 49–56.
[56] Y.L. Xu, L. Wang, M. Huang, F. Gensch, K.U. Kainer, N. Hort, Adv. Eng. Mater. 20 (2018) 1800271.